SCIENTIFIC PAPER

Study of continuous blood pressure estimation based on pulse transit time, heart rate and photoplethysmography-derived hemodynamic covariates

Jingjie Feng[1] · Zhongyi Huang[1] · Congcong Zhou[1] · Xuesong Ye[1,2]

Abstract

It is widely recognized that pulse transit time (PTT) can track blood pressure (BP) over short periods of time, and hemodynamic covariates such as heart rate, stiffness index may also contribute to BP monitoring. In this paper, we derived a proportional relationship between BP and PPT^{-2} and proposed an improved method adopting hemodynamic covariates in addition to PTT for continuous BP estimation. We divided 28 subjects from the Multi-parameter Intelligent Monitoring for Intensive Care database into two groups (with/without cardiovascular diseases) and utilized a machine learning strategy based on regularized linear regression (RLR) to construct BP models with different covariates for corresponding groups. RLR was performed for individuals as the initial calibration, while recursive least square algorithm was employed for the re-calibration. The results showed that errors of BP estimation by our method stayed within the Association of Advancement of Medical Instrumentation limits (-0.98 ± 6.00 mmHg @ SBP, 0.02 ± 4.98 mmHg @ DBP) when the calibration interval extended to 1200-beat cardiac cycles. In comparison with other two representative studies, Chen's method kept accurate (0.32 ± 6.74 mmHg @ SBP, 0.94 ± 5.37 mmHg @ DBP) using a 400-beat calibration interval, while Poon's failed (-1.97 ± 10.59 mmHg @ SBP, 0.70 ± 4.10 mmHg @ DBP) when using a 200-beat calibration interval. With additional hemodynamic covariates utilized, our method improved the accuracy of PTT-based BP estimation, decreased the calibration frequency and had the potential for better continuous BP estimation.

Keywords Blood pressure · Pulse transit time · Pulse wave velocity · Hemodynamic · MIMIC

Introduction

Blood pressure (BP) is one of the vital physiological parameters indicating people's health status about the elasticity of aortic wall, the pulsatile rhythm of cardiac output (CO) and other cardiovascular conditions. The normal resting systolic/diastolic blood pressure (SBP/DBP) for a healthy adult is approximately 120/80 mmHg. BP fluctuates depending on many situations such as emotion variation, exercise, drug intake and disease.

Since cardiovascular diseases (CVDs) are the leading causes of death globally [1, 2] and elevated BP is considered as a major risk factor for CVDs, BP monitoring attracts more and more attention in modern medical care. Although accurate BP measurement can be fulfilled by an invasive way (e.g. insertion of an intra-arterial catheter), which is usually adopted in the intensive care unit (ICU), there is still urgent requirement for noninvasive BP measurement methods. Oscillometric technique and auscultation method [3, 4] are two most common cuff-based ways to measure BP noninvasively. However, the pneumatic cuff around upper arm hinders the user from normal activities (e.g. the inflation disturbs sleep during night). The measurement reliability is also somehow challenged due to the occasional white coat syndrome [5]. More importantly, cuff-based methods only achieve the intermittent BP recording with periodic cuff inflation and deflation, which means they lack the capability to track sudden BP variations. Volume clamping method and applanation tonometry [6–11] provide continuous beat-to-beat BP monitoring. However, both methods require

✉ Xuesong Ye
  yexuesong@zju.edu.cn

1 Biosensor National Special Laboratory, College of Biomedical Engineering and Instrument Science, Zhejiang University, Hangzhou 310027, People's Republic of China

2 State Key Laboratory of CAD & CG, Zhejiang University, Hangzhou 310027, People's Republic of China

relatively cumbersome mechanical structures and are highly sensitive to the sensor placement.

Under this circumstance, the estimation of BP in successive cardiac cycles via pulse wave velocity (PWV) or pulse transit time (PTT) has been extensively introduced over the last decades [4, 12–25]. PTT is defined as the time duration for an arterial pressure pulse wave traveling from the proximal artery to the distal location and PWV refers to the speed at which the pressure wave propagates. The correlations of PTT to mean arterial blood pressure (MAP), SBP and DBP have been studied by many researchers. Linear [16, 17], logarithmical [18–20] and other nonlinear [21–25] relationships have been conducted. Furthermore, methods exploiting additional covariates (e.g. heart rate, PTT variability) have been proposed for better BP prediction [26–28]. Among those PTT-based methods, Chen's and Poon's algorithms [16, 18, 19] are the most representative [4, 29]. Chen et al. [16] deduced a linear relationship between SBP and PTT, while Poon and Zhang [18] found that MAP is logarithmically related to PTT. Although good correlations between PTT and BP have been derived, the aforementioned methods still need improvements, since BP is influenced by lots of factors (e.g. gender, age and hemodynamic parameters) rather than simple PTT [30–33]. Besides, the duration of calibration intervals which estimation errors stay within the Association of Advancement of Medical Instrumentation (AAMI) limits could be investigated, since the calibration frequency is another important concern apart from the estimation accuracy.

Herein, we aimed to improve the conventional PTT-based methods with increased accuracy and decreased calibration frequency. We used the Navier–Stokes equation to newly derive a proportional relationship between BP and PPT^{-2} and presented an improved method utilizing hemodynamic covariates in addition to PTT to prompt a better BP estimation. We collected study population from an open accessible database and constructed BP models for subjects with/without CVDs respectively. The selection of model covariates was based on the biological plausibility and significant correlations in univariate and multivariate analyses. Besides, we performed a machine learning strategy based on regularized linear regression (RLR) for BP models as the initial calibration and recursive least square (RLS) algorithm as the re-calibration. Afterwards, we verified our method against the AAMI standard and compared it with Chen's and Poon's algorithms.

Materials and methods

Theoretical background

Most PTT-based methods are formed on the basis of the Bramwell–Hill and Moens–Korteweg equations, and the exponential model of the Young's elastic modulus [4, 34–36], which can be expressed as Eqs. (1) and (2), respectively.

$$PWV = \frac{1}{\sqrt{L \times C}} = \sqrt{\frac{A \times dP}{\rho \times dA}} \tag{1}$$

$$PWV = \sqrt{\frac{ghE_i}{2\rho r}} = \sqrt{\frac{ghE_0 e^{\gamma P}}{2\rho r}} \tag{2}$$

Equation (1) shows that PWV is a function of compliance C, where C and blood pressure P are inversely related. $L = \rho/A$, represents the arterial inertance per unit length. ρ is the density of the blood, A is the cross-sectional area of the artery. Equation (2) shows that the elastic modulus of the artery wall E_i is related to PWV and E_i increases with P. r is the radius of the artery, h is the thickness of the wall, g represents the gravitational constant and E_0 is the elastic modulus at zero pressure.

As one of the representative studies in this area, Chen et al. [16] deduced the relationship between BP and PTT as Eq. (3).

$$P_E = P_b - \frac{2}{\gamma T_b} \Delta T \tag{3}$$

where P_E is the estimated BP, P_b is the initial BP value, T_b is the initial PTT value, γ is a coefficient depending on the particular vessel and ΔT is the change of PTT. Besides, Chen applied an adjustable bandpass filter to PTT data [known as the high frequency component (HFC)] and corrected P_E via a linear lookup table [noted as the low frequency component (LFC)] between the calibration points.

Poon and Zhang [18] developed a method based on a logarithmical BP–PTT relationship, as given in Eqs. (4) and (5).

$$DBP = \frac{SBP_0}{3} + \frac{2DBP_0}{3} + \frac{2}{\gamma} \ln\left(\frac{PTT_0}{PTT}\right)$$
$$- \frac{(SBP_0 - DBP_0)}{3}\left(\frac{PTT_0}{PTT}\right)^2 \tag{4}$$

$$SBP = DBP + (SBP_0 - DBP_0)\left(\frac{PTT_0}{PTT}\right)^2 \tag{5}$$

where SBP_0 and DBP_0 are the initial BP values, $\gamma = 0.031$ mmHg^{-1}, and PTT_0 is the initial PTT value.

In this study, a derivation of the relationship between BP and PTT was attempted from the Navier–Stokes equation (Eq. 6), which describes the motion of viscous fluid substances.

$$\frac{\partial \rho v_x}{\partial \tau} + \rho \left(v_x \frac{\partial v_x}{\partial x} + v_y \frac{\partial v_x}{\partial y} + v_z \frac{\partial v_x}{\partial z} \right)$$
$$= \mu \left[\frac{\partial}{\partial x} \left(\frac{\partial v_x}{\partial x} \right) + \frac{\partial}{\partial y} \left(\frac{\partial v_x}{\partial y} \right) + \frac{\partial}{\partial z} \left(\frac{\partial v_x}{\partial z} \right) \right] - \frac{\partial P}{\partial x} + \rho g$$

(6)

where ρ is the density of the fluid, μ is the viscosity, v is the flow velocity along its direction and g is the gravitational constant. The left side of the equation describes the time-dependent momentum and convective components, while the right side is a summation of divergence of deviatoric stress, hydrostatic effect (i.e. pressure) and gravity.

In this study, the blood is simplified as incompressible Newtonian fluid. The laminar blood flows from the heart to peripherals such that the density and viscosity of the blood are assumed to be constant during each calibration interval. Furthermore, blood in arteries is considered to flow only along the axial direction and the properties of arteries (e.g. cross-sectional area of artery, thickness of aortic wall) are thought to be constant. When integrating the Navier–Stokes equation for a steadily laminar flow, Eq. (7) is derived.

$$\frac{1}{2} \rho v^2 = (h_f + \rho g H) - P$$

(7)

where P is the BP, g is the gravitational constant, H stands for the height difference between two measurement sites, ρ is the density of blood, h_f is the energy loss due to the peripheral resistance of arteries, v is the velocity, which can be expressed as L/PTT and L is the distance along the artery. Kinetic energy changes at the expense of pressure energy. Once the placement of the sensors is fixed, H, L and h_f are regarded as constants during each calibration interval. BP can be obtained as Eq. (8), which shows a proportional relationship to PTT^{-2}.

$$BP = a + \frac{b}{PTT^2}$$

(8)

where a and b are coefficients.

In addition to PTT, hemodynamic factors could alter BP levels [37]. In order to achieve better BP estimation, we have taken hemodynamic covariates into consideration. They include (1) augmentation index (AIx), defined as the percentage of the central pulse amplitude which is attributed to the reflected pulse wave, is a measure of the wave reflection [38–40]; (2) stiffness index (SIx), which exhibits the time interval between an early systolic peak and a later diastolic peak, indicates the arterial stiffness [41]; (3) rise time (RT), which is associated with the contractile force and left ventricular function, is a time interval with respect to the steep rise of the arterial pressure from its nadir to a peak [42]; (4) pressure constant k (PK), calculated as the proportion of the mean pulsatile component in the maximum pulse pressure during a cardiac cycle, is related to the total peripheral resistance (TPR) [43]; (5) photoplethysmography area (PA), defined as a function of the areas under the PPG curve between certain points, could reflect TPR [44]; (6) descent time (DT) interpreted as the duration from the onset of the dicrotic notch to the end of the diastole [45]; (7) pulsatile hetero-height (PHH), which is a function of the pulse amplitude (Ppeak), RT and DT, is connected with CO. Some of these features are illustrated in Fig. 1.

Correlations of these covariates to BP are assessed by univariate and multivariate analyses. The BP models utilizing PTT^{-2} and hemodynamic covariates are constructed for groups with/without CVDs respectively. The coefficients of BP models are initiated by the initial calibration using RLR and adjusted by the re-calibration using RLS algorithm. The main processes of our method are summarized in Fig. 2, which will be elaborated as follows.

Data acquisition and study population

The multi-parameter Intelligent Monitoring for Intensive Care (MIMIC) database developed by the MIT Lab is used [46]. It includes signals (e.g. multi-lead electrocardiograms (ECGs), arterial blood pressure (ABP), photoplethysmograph (PPG) and respiration signal) and periodic measurements (e.g. heart rate (HR), oxygen saturation (SPO$_2$) and SBP/DBP/MAP) for different patients. Out of 72 records from 55 patients available, only the subject's records that contained continuous signals of interest (i.e. ECG, PPG and ABP) were included. The subjects who had obviously abnormal waveforms were excluded. Afterwards, the remaining 28 subjects were divided into two groups, according to the
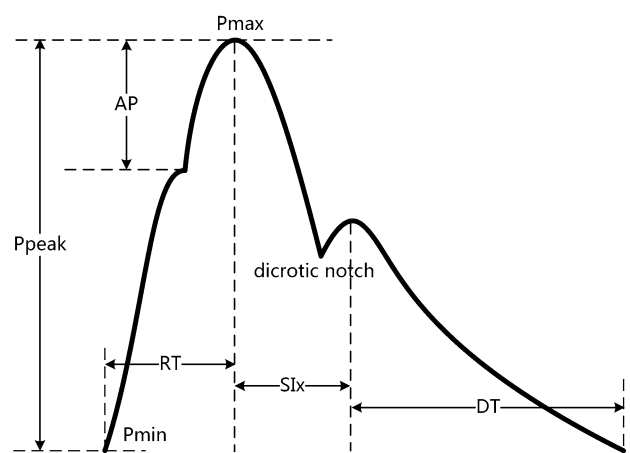

Fig. 1 Extraction of hemodynamic covariates. *Pmax* the peak of PPG signal, *Pmin* the nadir of PPG signal, *Ppeak* the pulse amplitude, *AP* augmented pulse caused by wave reflection. Augment index (AIx = AP/Ppeak×100), *RT* rise time, *SIx* stiffness index, *DT* descent time
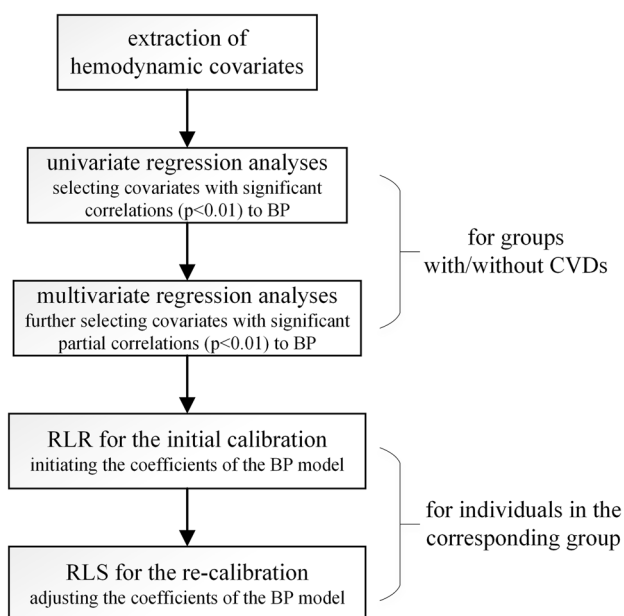
Fig. 2 The main schematic of our method

initial diagnoses with/without heart or CVDs when they were admitted to the ICU.

Signal preprocessing

Signals of interest were separated into small segments to improve the processing efficiency. Two adjacent segments were overlapped by 10 s intervals to avoid missing detection of feature points. Moreover, both ABP and PPG signals, which were recorded at 125 Hz, were re-sampled to 500 Hz by linear interpolation, in order to synchronize the result with the ECG signals which were originally sampled at 500 Hz. Afterwards, averaging filter and wavelet transform were performed on each signal segment. The ECG and PPG signals were decomposed to eight levels by Daubechies db5 wavelet function, then the corresponding approximate coefficients were low-pass filtered before signal reconstruction.

Feature extraction

ECG features

R peak of each filtered QRS complex was extracted by an unfixed-width sliding window and a dynamic adaptive threshold, HR was calculated from adjacent R–R interval.

PPG features

There were several feature points extracted, to be used as indicators of the pulse onset location. They include the PPG maximum/minimum peak (Pmax/Pmin) and the point

at which 20% amplitude of the PPG waveform appeared. PTT could be obtained in each cardiac cycle by calculating the time interval between the R peak of ECG signal and the corresponding characteristic point of PPG signal. Besides, the hemodynamic covariates mentioned above were also extracted. PTT, HR and other covariates were normalized by means of z-score method.

ABP features

ABP signal was used as the reference. The maximum and minimum peaks of the ABP signal in each R–R interval were considered as SBP and DBP, respectively.

Statistical analyses and model construction

Statistical analyses were conducted using SPSS. For each group (with/without CVDs), total and partial Pearson correlation coefficients were analyzed to estimate the correlations between BP and PTT^{-2}, together with those hemodynamic covariates. The significant level was set at $p < 0.01$. The selection of covariates to be included in multiple regression analyses was based on their clinical and biological plausibility and after significant correlations had been obtained in univariate regression analyses. Afterwards, the first three variables with the highest partial correlations in multiple regression analyses, were selected for model construction.

For each subject in the corresponding group, RLR was employed to initiate the coefficients of the model, which was regarded as the initial calibration. Mean squared error (MSE) was used as the cost function. The data was partitioned into three sets (i.e. training, cross validation and test set). Polynomial terms were added as extra features and regularization parameter was computed by the cross validation set.

Furthermore, the BP model needed intermittent re-calibration due to the time-varying properties of vascular parameters. Hence, RLS algorithm with the forgetting factor was adopted to adjust the coefficients of the model as the re-calibration process.

Evaluation of the proposed method

The proposed method was compared with Chen's and Poon's algorithms. The three algorithms were performed on the test set. The mean error and standard deviation (mean ± SD) were calculated and verified against the AAMI standard. All algorithms were evaluated as follows:

(1) Errors using each algorithm were calculated over different duration (200–1200 beats) after the initial calibra-

tion, and the duration that the estimated BP exceeded the AAMI limits for the first time was compared.

(2) The test set was separated into segments by a certain re-calibration interval (200–1200 beats). Estimation errors were averaged over all the segments using the three algorithms, and the longest duration that the estimated BP could remain accurate was compared.

Results

The selected 28 subjects were divided into two groups with/without CVDs. The PTT here was calculated as the duration from the R peak of ECG signal to the foot of PPG signal. The baseline clinical characteristics of the study population were displayed in Table 1.

Correlation coefficient values for each subject were averaged over their group to get population mean value. Univariate regression analyses showed a good correlation among PTT^{-2}, HR, RT, SIx, Pmax, etc, and SBP (r = 0.481, −0.277, 0.196, 0.239, 0.141; p < 0.01), the same as PTT^{-2}, HR, PK, SIx, DT, etc, and DBP (r = 0.457, −0.276, 0.141, 0.233,

−0.194; p < 0.01) in the subjects without CVDs. Among the subjects with CVDs, PTT^{-2}, HR, RT, AIx, Pmax, etc, was related to SBP (r = 0.471, −0.281, 0.35, 0.256, 0.254; p < 0.01), and PTT^{-2}, HR, PK, DT, SIx, etc, was associated with DBP (r = 0.411, −0.291, 0.218, −0.194, 0.179; p < 0.01). Subsequently, these covariates with significant correlations (p < 0.01) were included in the multivariate regression analyses, while covariates with insignificant correlations (e.g. PHH) were excluded. Pearson correlation coefficients of univariate regression analyses were revealed in Table 2.

The relationships between BP and selected hemodynamic covariates were investigated using multivariate stepwise linear regression analyses. Among the subjects without CVDs, PTT^{-2}, HR and SIx (β = 0.414, −0.211, 0.131; p < 0.01) were proved to be major determinants of SBP, while PTT^{-2}, HR and DT (β = 0.449, −0.22, −0.097; p < 0.01) for DBP. Meanwhile, among the subjects with CVDs, PTT^{-2}, HR and RT (β = 0.376, −0.168, 0.135; p < 0.01) made major contributions to SBP, while PTT^{-2}, HR and PK (β = 0.335, −0.141, 0.105; p < 0.01) for DBP. Table 3 demonstrated partial Pearson correlation coefficients of multivariate regression analyses.

After multivariate regression analyses, the first three variables with highest partial correlations were chosen for BP modeling. Table 4 summarized the variables finally selected for model construction.

Figure 3 exhibited the average errors for all the subjects over different intervals after the initial calibration. It was aimed to assess the longest duration that the estimated BP would remain accurate until a re-calibration was required. Once the initial calibration was completed, Chen's algorithm exceeded the AAMI limits after 600-beat duration (7.26 ± 1.12 min; error: 1.36 ± 8.31 mmHg @ SBP), while

Table 1 Baseline characteristics of the study population

	Subjects without CVDs	Subjects with CVDs
Number	15	13
Male (%)	53.3%	53.8%
Age (years)	72.7 ± 10.2	69.1 ± 18.6
SBP (mmHg)	119.5 ± 26.8	119.1 ± 27.1
DBP (mmHg)	58.4 ± 14.4	63.0 ± 19.8
PTT (s)	0.237 ± 0.055	0.203 ± 0.082
HR (bpm)	87.3 ± 14.7	89.4 ± 19.4

Table 2 Univariate linear regression analyses: correlations of BP to other variables

	Subjects without CVDs				Subjects with CVDs			
	SBP		DBP		SBP		DBP	
	r	p	r	p	r	p	r	p
PTT^{-2}	0.481	< 0.01	0.457	< 0.01	0.471	< 0.01	0.411	< 0.01
HR	− 0.277	< 0.01	− 0.276	< 0.01	− 0.281	< 0.01	− 0.291	< 0.01
RT	0.196	< 0.01	0.084	< 0.01	0.35	< 0.01	0.041	< 0.01
SIx	0.239	< 0.01	0.233	< 0.01	0.224	< 0.01	0.179	< 0.01
PK	0.091	< 0.01	0.141	< 0.01	0.134	< 0.01	0.218	< 0.01
DT	− 0.138	< 0.01	− 0.194	< 0.01	− 0.079	< 0.01	− 0.194	< 0.01
PHH	0.021	0.042	0.023	0.029	− 0.02	0.046	0.023	0.018
AIx	0.134	< 0.01	0.137	< 0.01	0.256	< 0.01	0.126	< 0.01
PA	0.092	< 0.01	0.143	< 0.01	0.177	< 0.01	0.117	< 0.01
Ppeak	0.076	< 0.01	0.051	< 0.01	0.047	< 0.01	0.05	< 0.01
Pmax	0.141	< 0.01	0.01	0.354	0.254	< 0.01	0.031	< 0.01
Pmin	− 0.008	0.522	− 0.13	< 0.01	0.014	0.157	0.158	< 0.01

Table 3 Multivariate linear regression analyses: correlations of BP to other variables

	Subjects without CVDs				Subjects with CVDs			
	SBP		DBP		SBP		DBP	
	β	p	β	p	β	p	β	p
PTT^{-2}	0.414	<0.01	0.449	<0.01	0.376	<0.01	0.335	<0.01
HR	−0.211	<0.01	−0.22	<0.01	−0.168	<0.01	−0.141	<0.01
RT	0.092	<0.01	–	–	0.135	<0.01	–	–
SIx	0.131	<0.01	0.086	<0.01	0.078	<0.01	0.073	<0.01
PK	–	–	–	–	0.037	<0.01	0.105	<0.01
DT	−0.021	<0.01	−0.097	<0.01	−0.031	<0.01	−0.086	<0.01
PHH	–	–	–	–	–	–	–	–
AIx	0.058	<0.01	0.072	<0.01	0.089	<0.01	0.043	<0.01
PA	–	–	–	–	0.047	<0.01	0.036	<0.01
Ppeak	0.033	<0.01	–	–	–	–	–	–
Pmax	0.088	<0.01	–	–	0.086	<0.01	–	–
Pmin	–	–	−0.045	<0.01	–	–	0.051	<0.01

Table 4 The selection of variables for BP models

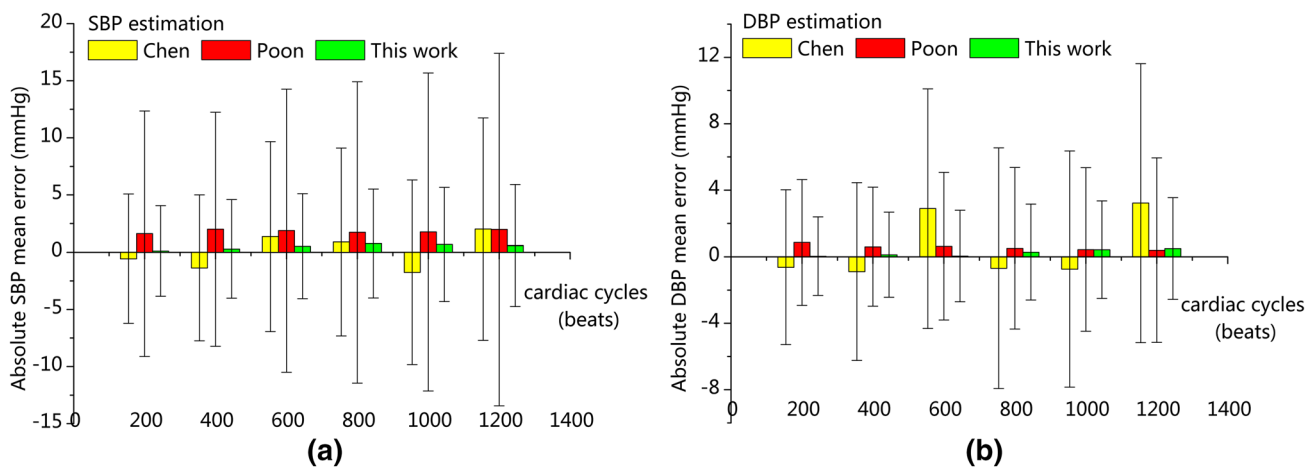|	Subjects without CVDs		Subjects with CVDs	
	SBP	DBP	SBP	DBP
Variables	PTT^{-2}, HR, SIx	PTT^{-2}, HR, DT	PTT^{-2}, HR, RT	PTT^{-2}, HR, PK

Fig. 3 **a** Errors of SBP estimation and **b** errors of DBP estimation, using the three algorithms over different duration (200–1200 beats) after the initial calibration. The errors were averaged over all the subjects

Poon's algorithm failed to satisfy the standard after a duration of 200 beats (2.42 ± 0.40 min; error: 1.61 ± 10.74 mmHg @ SBP). In contrast, our algorithm performed at the longest duration before the first re-calibration and the estimated BP kept accurate within a 1200-beat interval (14.54 ± 2.41 min; error: 0.58 ± 5.33 mmHg @ SBP).

Large SBP fluctuations were also observed in some subjects, which meant that the re-calibration interval should be adjusted to compromise the estimation accuracy. Taking subject no. 252 in the MIMIC database as an example

(Fig. 4), SBP estimated by our method (red line) coordinated better with ABP (blue line) than that estimated by Chen's and Poon's algorithms (orange and green lines) when a 600-beat calibration interval was applied. ABP kept steady at 105.73 ± 4.22 mmHg for the first 600-beat interval, then it rose progressively to 136.17 ± 2.98 mmHg at 4200–4800 beats. Afterwards, ABP dropped sharply from 110.38 ± 2.02 mmHg (6300–6600 beats) to 89.62 ± 4.19 mmHg (6601–6900 beats). Hence, for the subjects that had considerable BP variations, the required

re-calibration interval might differ from the duration that the estimated BP first exceeded the AAMI limits after the initial calibration.

Furthermore, the effect of different re-calibration intervals (200–1200 beats) were evaluated and the results were shown in Fig. 5. Generally, shorter re-calibration interval improved the accuracy at the cost of inconvenience. Although a re-calibration interval of 400 beats (4.83 ± 0.80 min; errors: 0.32 ± 6.74 mmHg @ SBP, 0.94 ± 5.37 mmHg @ DBP) was sufficient for Chen's algorithm, a less than 200-beat re-calibration interval was required for Poon's algorithm (errors: -1.97 ± 10.59 mmHg @ SBP, 0.70 ± 4.10 mmHg @ DBP, using a 200-beat interval). The forgetting factor of the RLS algorithm in our model was set as 0.98 and the corresponding estimated BP successfully maintained accurate within a 1200-beat re-calibration interval (14.54 ± 2.41 min; errors: -0.98 ± 6.00 mmHg @ SBP, 0.02 ± 4.98 mmHg

@ DBP), which has the longest duration among the three algorithms. Also, the estimated DBP had smaller deviations from ABP than the estimated SBP for all the re-calibration intervals in the three algorithms.

Discussion

This study proposed an evaluation of the feasibility of continuous BP estimation based on PTT and other hemodynamic covariates through a set of patient's clinical signals available on the MIMIC database. Many studies as well as our own findings have supported the idea that a good correlation exists between BP and PTT/PWV. For most of these studies, the Bramwell–Hill and Moens–Korteweg equations have provided the basic mathematical foundation for the PTT–BP relationship. In contrast, we derived their relationship from the Navier–Stokes equation, which describes the momentum conservation in incompressible fluids. In addition to this, hemodynamic covariates and PTT have been employed in the BP modeling such that selection of the covariates was separately conducted for groups of subjects with/without CVDs.

As one of the representative studies in the area of PTT-based BP estimation, Chen found a calibration interval of 5 min was sufficient in his work. And our result showed that Chen's algorithm remained accurate using a 400-beat calibration interval (4.83 ± 0.80 min among 28 subjects as shown in Fig. 5). It should be pointed out that Chen's algorithm adopted a combination of the HFC and LFC. The HFC was used to filter the data via a digital bandpass filter whose cut-off frequency was adjusted according to different calibration intervals. The LFC was a look-up table which was realized by a linear interpolation method and was measured
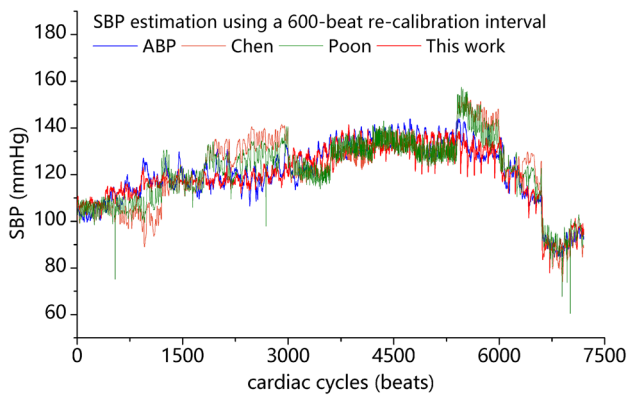

Fig. 4 SBP estimation of subject no. 252 using a 600-beat re-calibration interval
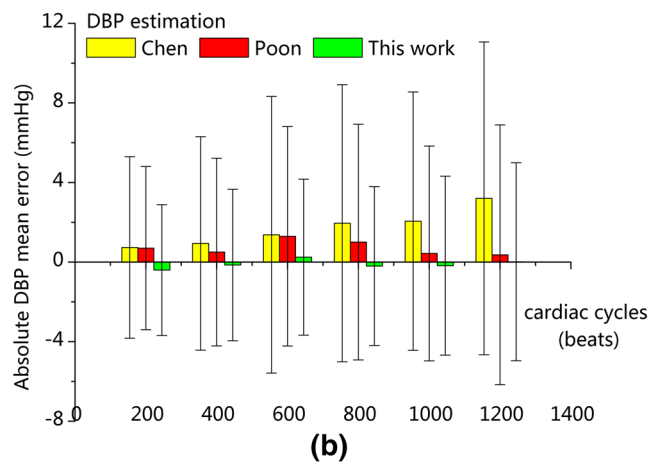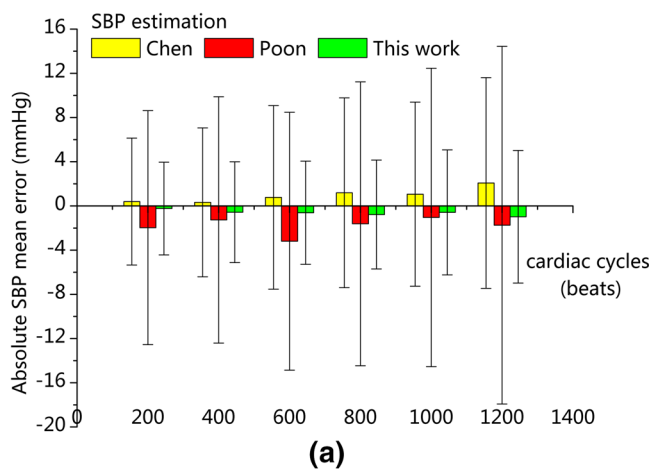

Fig. 5 a Errors of SBP estimation and **b** errors of DBP estimation, using the three algorithms via different re-calibration intervals (200–1200 beats). The errors were averaged over the whole test set and all the subjects

from the calibration points. Due to the bandpass filtering, the estimated BP would not fluctuate wildly in each calibration interval. As illustrated in Fig. 4, the SBP estimated by Chen's algorithm (orange line) coordinated with ABP (blue line) when ABP did not change much (e.g. intervals of 1–600, 3601–4200 and 4201–4800 beats). However, the estimated SBP failed to catch up with ABP when ABP greatly altered (e.g. intervals of 601–1200 and 5401–6600 beats). It appeared that Chen's method could accurately predict BP if it did not vary rapidly. Owing to the requirement of the LFC to diminish errors, BP estimated by Chen's method was not provided in real time, but with a time delay which was equivalent to the calibration interval. Alternatively, Poon's algorithm exceeded the AAMI limits even when a 200-beat calibration interval (2.42 ± 0.40 min) was adopted, and this result was in accordance with what Poon had found in his work. It was plausible that small errors in PTT measurement could cause large errors in BP estimation due to their logarithmic relationship. Those outliers (Fig. 4) also contributed to the large SD of Poon's algorithm.

In order to further improve the BP estimation and according to the suggestions that additional covariates such as HR could help address this problem [4, 29], the utilization of hemodynamic covariates was attempted for this purpose. In our method, the selected covariates was based on their clinical and biological plausibility. Among them, HR was strongly affected by the baroreflex regulation, which played a role in maintaining BP despite large alterations. Baroreceptor-sensed BP fluctuations provoked RR interval variability [26, 27, 47–50]. SIx was an important indicator of the arterial stiffness [41]. RT was associated with the contractile force and left ventricular function [51]. PK could reflect the arterial compliance and peripheral resistance [43]. DT was related to the diastolic phase of the cardiac cycle. These covariates could somewhat reflect the cardiovascular functions and were associated with BP variations. Moreover, Tanaka et al. [37] found that significant hemodynamic determinants of SBP included arterial stiffness, left ventricular ejection fraction and arterial wave reflection, while DBP was primarily govern by peripheral resistance, HR and arterial stiffness. These relationships were demonstrated in Fig. 6. Our results also proved that the aforementioned hemodynamic covariates adopted in our model (listed in Table 4) effectively improved the accuracy and extended the calibration interval.

Another concern was that the selection of different feature points used as the pulse onsets of PPG would influence the correlation of PTT to BP. Other researchers had found good correlations between PTT and BP using various characteristic points, such as peak (the maximum of PPG) [29], foot (the minimum of PPG) [52, 53], the maximal slope point on the rising edge [54, 55], the location of the maximum second derivative [56] and the tangent intersection point

[57]. We found that the PTT derived from the foot correlated slightly better with BP than the PTT obtained from the 20% amplitude of PPG signal, while the PTT calculated from the peak correlated poorly with BP (data not shown). This result could be explained as the impact of the wave reflection that distorted distal waveforms morphologically. The PTT determined from the peak was then contaminated and was prone to miscalculation when using the peak as the pulse onset of PPG. Mukkamala et al. [4] and Lillie et al. [53] also concluded that the foot of the pulse waveform denoted the preferred feature for detection and the wave reflection interference was small at the minimum or foot. Moreover, the PTT in this approach, whose nomenclature was actually the pulse arrival time (PAT), employed ECG as a surrogate for the proximal pulse wave. This duration contained a non-ignorable fraction called the pre-ejection period (PEP). PEP was determined by the ventricular electromechanical delay and isovolumic contraction period [12, 58], which was modulated by medication, short-term physiologic control and smooth muscle contraction [59, 60]. Hence, PAT had an imprecise relationship with BP according to Eqs. (1), (2), and (8), since its PEP proportion might change considerably [61]. In addition to this, the fluctuation of SBP was usually greater than DBP [4, 62], resulting in a larger SD in SBP estimation. It could explain the phenomenon in Figs. 3 and 5 that the estimated SBP deviated from ABP more than the estimated DBP.

Despite the improvements in estimation accuracy and calibration frequency, there were still some limitations of our method. Only 28 subjects were studied and the small amount of subjects constrained the significance of the results. The data used here were recorded from the patients in ICU and medications were provided to each subject. Although drug intake might cause different cardiovascular
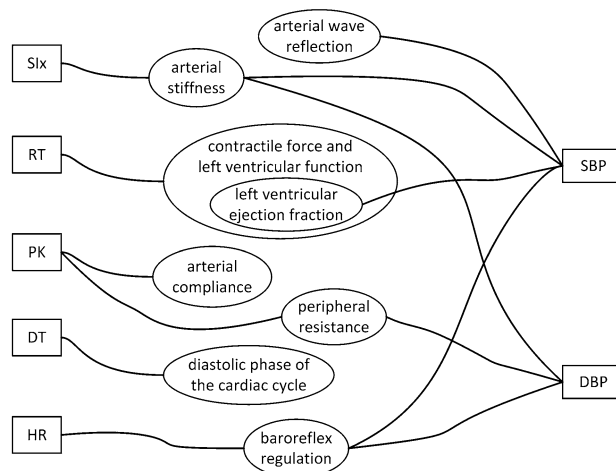

Fig. 6 The relationships between BP and the hemodynamic covariates

responses and vary BP, the impact of this phenomenon was not taken into account. In addition, the actual arterial system consisted of branches rather than a simple tube. The PTT–BP relationship attenuated at peripheral arteries where vasomotion was present [63]. Besides, elastic and muscular arteries differed in biomechanical properties according to their composition of arterial walls, which could alter the modulation of blood flow and arterial elasticity and affect the PTT–BP relationship [4]. Therefore, factors such as vasomotion in distal arterial trees and the biomechanical properties of arteries where pulse waves propagated were worthy to notice.

In this study, our model was initially fitted on the training set. The regression model was then tuned on the validation set, which was used for regularization to avoid overfitting. Tenfold cross validation was adopted to provide an unbiased evaluation of BP modeling and decide the final model parameters. There might be a burden of requiring more training data, since our model was characterized by more variables than Chen's and Poon's algorithms. Nonetheless, collecting enough data for model construction was necessary to enhance the accuracy, especially for the machine learning strategies which were more complex than ours [e.g. artificial neural network (ANN) and support vector regression (SVR)]. High accuracy could be acquired by increasing the number of hidden units or using specific kernel function, while sufficient training data improved the performance (i.e. generalization) of the model with minimal overfitting. In our method, all the variables could be acquired by only two sensors, namely the ECG and PPG sensors, and no extra hardware resources were required. It was acceptable if the accuracy increased without significantly compromising the convenience (i.e. the endeavor to gather necessary data for model construction).

Conclusion

An improved continuous BP estimation method utilizing hemodynamic covariates in addition to PTT was proposed for the subjects in the MIMIC database. It demonstrated that this method had the potential to continuously track BP with more accuracy and less calibration frequency. Nevertheless, more validation in various subjects and situations should be conducted before practical applications of this study.

Compliance with ethical standards

Conflict of interest The authors declare that they have no conflict of interest.

Ethical approval This article does not contain any studies with human participants performed by any of the authors. The datasets analysed during the current study are available in the PhysioNet repository, https://physionet.org/physiobank/database/mimicdb/.

References

1. Mendis S, Puska P, Norrving B (2011) Global atlas on cardiovascular disease prevention and control. World Health Organization, Geneva
2. Mancia G, Fagard R, Narkiewicz K, Redon J, Zanchetti A, Böhm M et al (2013) 2013 ESH/ESC guidelines for the management of arterial hypertension: the Task Force for the Management of Arterial Hypertension of the European Society of Hypertension (ESH) and of the European Society of Cardiology (ESC). Blood Press 22(4):193–278
3. Peter L, Noury N, Cerny M (2014) A review of methods for non-invasive and continuous blood pressure monitoring: pulse transit time method is promising? Irbm 35(5):271–282
4. Mukkamala R, Hahn J-O, Inan OT, Mestha LK, Kim C-S, Töreyin H et al (2015) Toward ubiquitous blood pressure monitoring via pulse transit time: theory and practice. IEEE Trans Biomed Eng 62(8):1879–1901
5. O'Brien E, Asmar R, Beilin L, Imai Y, Mallion J-M, Mancia G et al (2003) European Society of Hypertension recommendations for conventional, ambulatory and home blood pressure measurement. J Hypertens 21(5):821–848
6. Dueck R, Goedje O, Clopton P (2012) Noninvasive continuous beat-to-beat radial artery pressure via TL-200 applanation tonometry. J Clin Monit Comput 26(2):75–83
7. Lee B, Jeong J, Kim J, Kim B, Chun K (2014) Cantilever arrayed blood pressure sensor for arterial applanation tonometry. IET Nanobiotechnol 8(1):37–43
8. Saugel B, Dueck R, Wagner JY (2014) Measurement of blood pressure. Best Pract Res Clin Anaesthesiol 28(4):309–322
9. Imholz BP, Wieling W, van Montfrans GA, Wesseling KH (1998) Fifteen years experience with finger arterial pressure monitoring: assessment of the technology. Cardiovasc Res 38(3):605–616
10. Wesseling K, De Wit B, Van der Hoeven G, Van Goudoever J, Settels J (1995) Physiocal, calibrating finger vascular physiology for Finapres. Homeost Health Dis 36(2–3):67
11. Sato T, Nishinaga M, Kawamoto A, Ozawa T, Takatsuji H (1993) Accuracy of a continuous blood pressure monitor based on arterial tonometry. Hypertension 21(6 Pt 1):866–874
12. Dilpreet B, Jean-Michel R, Mehmet Rasit Y (2015) A survey on signals and systems in ambulatory blood pressure monitoring using pulse transit time. Physiol Meas 36(3):R1–R26
13. Can Y, Kilic H, Akdemir R, Acar B, Edem E, Kocyigit I et al (2016) An investigation of pulse transit time as a blood pressure measurement method in patients undergoing carotid artery stenting. Blood Press Monit 21(3):168–170
14. Poon CC, Zhang Y-T, Liu Y (2006) Modeling of pulse transit time under the effects of hydrostatic pressure for cuffless blood pressure measurements. In: 3rd IEEE/EMBS international summer school on medical devices and biosensors, pp 65–68
15. Lopez G, Shuzo M, Ushida H, Hidaka K, Yanagimoto S, Imai Y et al (2010) Continuous blood pressure monitoring in daily life. J. Adv. Mech. Des. Syst. Manuf. 4(1):179–186

16. Chen MW, Kobayashi T, Ichikawa S, Takeuchi Y, Togawa T (2000) Continuous estimation of systolic blood pressure using the pulse arrival time and intermittent calibration. Med Biol Eng Comput 38(5):569–574

17. Escobar B, Torres R (2014) Feasibility of non-invasive blood pressure estimation based on pulse arrival time: a MIMIC database study. In: Computing in cardiology 2014, 7–10 Sept 2014, pp 1113–1116

18. Poon CCY, Zhang YT (2005) Cuff-less and noninvasive measurements of arterial blood pressure by pulse transit time. In: 2005 IEEE Engineering in Medicine and Biology 27th annual conference, 17–18 Jan 2006, pp 5877–5880)

19. Zheng YL, Yan BP, Zhang YT, Poon CCY (2014) An armband wearable device for overnight and cuff-less blood pressure measurement. IEEE Trans Biomed Eng 61(7):2179–2186

20. Puke S, Suzuki T, Nakayama K, Tanaka H, Minami S (2013) Blood pressure estimation from pulse wave velocity measured on the chest. In: 2013 35th annual international conference of the IEEE Engineering in Medicine and Biology Society (EMBC), 3–7 July 2013, pp 6107–6110

21. Gesche H, Grosskurth D, Küchler G, Patzak A (2012) Continuous blood pressure measurement by using the pulse transit time: comparison to a cuff-based method. Eur J Appl Physiol 112(1):309–315

22. Zheng DC, Murray A (2009) Non-invasive quantification of peripheral arterial volume distensibility and its non-linear relationship with arterial pressure. J Biomech 42(8):1032–1037

23. Chen Y, Wen CY, Tao GC, Bi M, Li GQ (2009) Continuous and noninvasive blood pressure measurement: a novel modeling methodology of the relationship between blood pressure and pulse wave velocity. Ann Biomed Eng 37(11):2222–2233

24. Zhang G, Gao M, Xu D, Olivier NB, Mukkamala R (2011) Pulse arrival time is not an adequate surrogate for pulse transit time as a marker of blood pressure. J Appl Physiol 111(6):1681–1686

25. Muehlsteff J, Aubert X, Schuett M (2006) Cuffless estimation of systolic blood pressure for short effort bicycle tests: the prominent role of the pre-ejection period. In: 28th annual international conference of the IEEE Engineering in Medicine and Biology Society, 2006 (EMBS'06), pp 5088–5092

26. Jadooei A, Zaderykhin O, Shulgin VI (2013) Adaptive algorithm for continuous monitoring of blood pressure using a pulse transit time. In: 2013 IEEE XXXIII international scientific conference electronics and nanotechnology (ELNANO), 16–19 April 2013, pp 297–301

27. Cattivelli FS, Garudadri H (2009) Noninvasive cuffless estimation of blood pressure from pulse arrival time and heart rate with adaptive calibration. In: 2009 sixth international workshop on wearable and implantable body sensor networks, 3–5 June 2009, pp 114–119

28. Ma HT (2014) A blood pressure monitoring method for stroke management. Biomed Res Int 2014:7

29. McCarthy B, Vaughan C, O'Flynn B, Mathewson A, Mathúna C (2013) An examination of calibration intervals required for accurately tracking blood pressure using pulse transit time algorithms. J Hum Hypertens 27(12):744–750

30. Mitchell GF, Parise H, Benjamin EJ, Larson MG, Keyes MJ, Vita JA et al (2004) Changes in arterial stiffness and wave reflection with advancing age in healthy men and women: the Framingham Heart Study. Hypertension 43(6):1239–1245

31. Foo JYA, Lim CS (2006) Pulse transit time as an indirect marker for variations in cardiovascular related reactivity. Technol Health Care 14(2):97–108

32. Schiffrin EL (2004) Vascular stiffening and arterial complianceImplications for systolic blood pressure. Am J Hypertens 17(S3):39S–48S

33. Yamashina A, Tomiyama H, Arai T, Koji Y, Yambe M, Motobe H et al (2003) Nomogram of the relation of brachial-ankle pulse wave velocity with blood pressure. Hypertens Res 26(10):801–806

34. Hughes DJ, Babbs CF, Geddes LA, Bourland JD (1979) Measurements of Young's modulus of elasticity of the canine aorta with ultrasound. Ultrason Imaging 1(4):356–367

35. Nichols W, O'Rourke M, Vlachopoulos C (2011) McDonald's blood flow in arteries: theoretical, experimental and clinical principles. Hodder Arnold, London

36. Geddes LA, Voelz M, James S, Reiner D (1981) Pulse arrival time as a method of obtaining systolic and diastolic blood pressure indirectly. Med Biol Eng Comput 19(5):671–672

37. Tanaka H, Heiss G, McCabe EL, Meyer ML, Shah AM, Mangion JR et al (2016) Hemodynamic correlates of blood pressure in older adults: the Atherosclerosis Risk in Communities (ARIC) Study. J Clin Hypertens 18(12):1222–1227

38. Nürnberger J, Keflioglu-Scheiber A, Saez AMO, Wenzel RR, Philipp T, Schäfers RF (2002) Augmentation index is associated with cardiovascular risk. J Hypertens 20(12):2407–2414

39. Davies JI, Struthers AD (2003) Pulse wave analysis and pulse wave velocity: a critical review of their strengths and weaknesses. J Hypertens 21(3):463–472

40. Kelly R, Hayward C, Avolio A, O'rourke M (1989) Noninvasive determination of age-related changes in the human arterial pulse. Circulation 80(6):1652–1659

41. Millasseau S, Kelly R, Ritter J, Chowienczyk P (2002) Determination of age-related increases in large artery stiffness by digital pulse contour analysis. Clin Sci 103(4):371–377

42. Zaidi SN, Collins SM (2016) Orthostatic stress and area under the curve of photoplethysmography waveform. Biomed Phys Eng Express 2(4):045006

43. Voelz M (1981) Measurement of the blood-pressure constant k, over a pressure range in the canine radial artery. Med Biol Eng Comput 19(5):535–537

44. Elgendi M (2012) On the analysis of fingertip photoplethysmogram signals. Curr Cardiol Rev 8(1):14–25

45. Esper SA, Pinsky MR (2014) Arterial waveform analysis. Best Pract Res Clin Anaesthesiol 28(4):363–380

46. Moody GB, Mark RG (1996) A database to support development and evaluation of intelligent intensive care monitoring. In: Computers in cardiology 1996, 8–11 Sept 1996, pp 657–660

47. Pitzalis MV, Mastropasqua F, Massari F, Passantino A, Colombo R, Mannarini A et al (1998) Effect of respiratory rate on the relationships between RR interval and systolic blood pressure fluctuations: a frequency-dependent phenomenon. Cardiovasc Res 38(2):332–339

48. Bernardi L, Leuzzi S, Radaelli A, Passino C, Johnston JA, Sleight P (1994) Low-frequency spontaneous fluctuations of RR interval and blood pressure in conscious humans: a baroreceptor or central phenomenon? Clin Sci 87(6):649–654

49. Wang R, Jia W, Mao ZH, Sclabassi RJ, Sun M (2014) Cuff-free blood pressure estimation using pulse transit time and heart rate. In 2014 12th international conference on signal processing (ICSP), 19–23 Oct 2014, pp 115–118

50. Reusz GS, Cseprekal O, Temmar M, Kis É, Cherif AB, Thaleb A et al (2010) Reference values of pulse wave velocity in healthy children and teenagers. Hypertension 56(2):217–224

51. Tartiere JM, Logeart D, Beauvais F, Chavelas C, Kesri L, Tabet JY et al (2007) Non-invasive radial pulse wave assessment for the evaluation of left ventricular systolic performance in heart failure. Eur J Heart Fail 9(5):477–483

52. Lopez G, Ushida H, Hidaka K, Shuzo M, Delaunay JJ, Yamada I et al (2009) Continuous blood pressure measurement in daily activities. In: 2009 IEEE sensors, 25–28 Oct 2009, pp 827–831

53. Lillie JS, Liberson AS, Borkholder DA (2016) Improved blood pressure prediction using systolic flow correction of pulse wave velocity. Cardiovasc Eng Technol 7:439–447

54. Yoon Y, Cho JH, Yoon G (2009) Non-constrained blood pressure monitoring using ECG and PPG for personal healthcare. J Med Syst 33(4):261–266

55. Wibmer T, Denner C, Fischer C, Schildge B, Rudiger S, Kropf-Sanchen C et al (2015) Blood pressure monitoring during exercise: comparison of pulse transit time and volume clamp methods. Blood Press 24(6):353–360

56. Mitchell GF, Pfeffer MA, Finn PV, Pfeffer JM (1997) Comparison of techniques for measuring pulse-wave velocity in the rat. J Appl Physiol 82(1):203–210

57. Chiu YC, Arand PW, Shroff SG, Feldman T, Carroll JD (1991) Determination of pulse wave velocities with computerized algorithms. Am Heart J 121(5):1460–1470

58. Harris WS, Schoenfeld CD, Weissler AM (1967) Effects of adrenergic receptor activation and blockade on the systolic preejection period, heart rate, and arterial pressure in man. J Clin Investig 46(11):1704–1714

59. Liu Q, Yan BP, Yu C-M, Zhang Y-T, Poon CC (2014) Attenuation of systolic blood pressure and pulse transit time hysteresis during exercise and recovery in cardiovascular patients. IEEE Trans Biomed Eng 61(2):346–352

60. Muehlsteff J, Aubert XA, Morren G (2008) Continuous cuffless blood pressure monitoring based on the pulse arrival time approach: the impact of posture. In: 2008 30th annual international conference of the IEEE Engineering in Medicine and Biology Society, 20–25 Aug 2008, pp 1691–1694

61. Payne R, Symeonides C, Webb D, Maxwell S (2006) Pulse transit time measured from the ECG: an unreliable marker of beat-to-beat blood pressure. J Appl Physiol 100(1):136–141

62. Virtanen R, Jula A, Kuusela T, Airaksinen J (2004) Beat-to-beat oscillations in pulse pressure. Clin Physiol Funct Imaging 24(5):304–309

63. Sola J, Proenca M, Ferrario D, Porchet J-A, Falhi A, Grossenbacher O et al (2013) Noninvasive and nonocclusive blood pressure estimation via a chest sensor. IEEE Trans Biomed Eng 60(12):3505–3513